A Close Quasar Pair in a Disk-Disk Galaxy Merger at $z = 2.17$

Yu-Ching Chen[1,2], Xin Liu[1,2], Adi Foord[3], Yue Shen[1,2], Masamune Oguri[4,5], Nianyi Chen[6], Tiziana Di Matteo[6,7,8], Miguel Holgado[6], Hsiang-Chih Hwang[9], Nadia Zakamska[10]

[1]*Department of Astronomy, University of Illinois at Urbana-Champaign, Urbana, IL 61801, USA*

[2]*National Center for Supercomputing Applications, University of Illinois at Urbana-Champaign, 605 East Springfield Avenue, Champaign, IL 61820, USA*

[3]*Kavli Institute of Particle Astrophysics and Cosmology, Stanford University, Stanford, CA 94305, USA*

[4]*Center for Frontier Science, Chiba University, Chiba 263-8522, Japan*

[5]*Department of Physics, Graduate School of Science, Chiba University, Chiba 263-8522, Japan*

[6]*McWilliams Center for Cosmology, Department of Physics, Carnegie Mellon University, Pittsburgh, PA 15213, USA*

[7]*NSF AI Planning Institute for Physics of the Future, Carnegie Mellon University, Pittsburgh, PA 15213, USA*

[8]*OzGrav-Melbourne, Australian Research Council Centre of Excellence for Gravitational*

Wave Discovery, Melbourne, VIC 3122, Australia

[9]*School of Natural Sciences, Institute for Advanced Study, Princeton, 1 Einstein Drive, NJ 08540, USA*

[10]*Department of Physics and Astronomy, Johns Hopkins University, Baltimore, MD 21218, USA*

Galaxy mergers produce pairs of supermassive black holes (SMBHs), which may be witnessed as dual quasars if both SMBHs are rapidly accreting. The kiloparsec (kpc)-scale separation represents a physical regime close enough for merger-induced effects to be important[1] yet wide enough to be directly resolvable with current facilities. While many kpc-scale dual active galactic nuclei – the low-luminosity counterparts of quasars – have been observed in low-redshift mergers[2], no unambiguous dual quasar is known at cosmic noon ($z \sim 2$), the peak of global star formation and quasar activity[3,4]. Here we report multi-wavelength observations of SDSS J0749+2255 as a kpc-scale dual quasar system hosted by a galaxy merger at cosmic noon ($z = 2.17$). We discover extended host galaxies associated with the much brighter compact quasar nuclei (separated by 0.″46 or 3.8 kpc) and low surface brightness tidal features as evidence for galactic interactions. Unlike their low-redshift and low-luminosity counterparts, SDSS J0749+2255 is hosted by massive compact disk-dominated galaxies. The apparent lack of stellar bulges and that SDSS J0749+2255 already follows

the local SMBH mass–host stellar mass relation suggest that at least some SMBHs may have formed before their host stellar bulges. While still at kpc-scale separations where the host-galaxy gravitational potential dominates, the two SMBHs may evolve into a gravitationally bound binary system in ∼0.22 Gyr.

SDSS J0749+2255 is an optically selected type 1 (i.e., broad-line) quasar at $z = 2.17$ spectroscopically confirmed by the SDSS legacy survey[5]. It was selected as a candidate kpc-scale dual quasar using Gaia astrometry[6]. *HST* optical dual-band imaging of SDSS J0749+2255 has revealed compact double nuclei with a projected nuclear angular separation of $0\farcs46$ (ref [7]). Close compact optical double nuclei could represent a dual quasar, a projected quasar pair in two non-interacting galaxies, a strongly lensed quasar, or a star-quasar superposition. Previous Very Long Baseline Array (VLBA) 15.0 GHz (Ku-band) imaging detected strong radio emissions from both nuclei, ruling out star-quasar superposition[7]. While morphological differences in the VLBA 15.0 GHz image of the two radio nuclei favor a dual quasar or a pre-merger projected quasar pair at larger physical separations, strong lensing could not be conclusively ruled out[7].

To unambiguously test the nature of SDSS J0749+2255, we have conducted a comprehensive multi-wavelength follow-up campaign. The new observations include *HST* IR F160W (H band) imaging, Keck adaptive optics (AO) assisted IR (K_p band) imaging,

HST/STIS optical spatially resolved slit spectroscopy, Gemini spatially resolved optical (GMOS) and NIR (GNIRS) slit spectroscopy, *Chandra* ACIS-S X-ray 0.5–8 keV imaging spectroscopy, and *Very Large Array* (*VLA*) A-configuration (A-config) radio dual-band (15 GHz and 6 GHz) imaging. These multi-wavelength observations establish SDSS J0749+2255 as a dual quasar hosted by an ongoing galaxy merger at $z = 2.17$.

First, after we subtract the bright central quasars modeled by two point-spread functions (PSFs), the deep *HST* IR image uncovers two extended host galaxies underlying both compact quasar nuclei (Figure 1). In addition, after we further subtract the best axisymmetric models for the extended host galaxies, the final residual image reveals low surface-brightness tidal features indicative of mergers (Figure 1). The detection of the faint tidal features is at high significance ($> 10\sigma$ for each integrated feature, SI). Detecting both the tidal features and the extended host galaxies unambiguously confirms SDSS J0749+2255 as a dual quasar in a merger rather than a strongly lensed quasar or a pre-merger projected quasar pair at larger physical separations. Complementary higher angular-resolution Keck AO-assisted IR imaging independently supports the detection of the extended host galaxies and the non-detection of a central foreground lens galaxy. The alternative scenario of a foreground lens galaxy as a single extended source located in between two compact quasar nuclei is quantitatively ruled out by strong lensing mass model tests (SI). However, the tidal features seen in the *HST* image are too faint to detect in the shallower Keck AO

image.

Second, *Chandra* ACIS-S detects both quasar nuclei in the hard X-rays (2–8 keV) as compact X-ray point sources whose spatial profiles are consistent with the PSF (Figure 2). The X-ray positional offsets between the two nuclei are consistent with those of the *HST* optical nuclei. The optically fainter NE nucleus is brighter in the X-rays than the SW nucleus. This contradicts naive expectations from a strongly lensed quasar, since gravitational lensing is in general achromatic: the deflection angle of a light ray (and the lensing magnification) does not depend on its wavelength so that consistent flux ratios are expected at different wavelengths from different lensed images given the same underlying source spectrum. While the wavelength-dependent geometry of the different emission regions may result in chromatic effects[8], the differences in the flux ratios between different images at different wavelengths should be minor in a strongly lensed quasar. However, the 2–8 keV X-ray flux ratio between the two nuclei (NE/SW) is 45^{+41}_{-33}, which is significantly different from that observed by *HST* in the optical (0.229 ± 0.001 in F475W and 0.284 ± 0.002 in F814W), disfavoring strong lensing. A caveat is that microlensing can cause such flux ratio anomalies given the different optical and X-ray emitting region sizes, which have been frequently observed[9–11], although the discrepancy for SDSS J0749+2255 is seen as extreme. The X-ray-to-optical luminosity ratio typically characterized by the spectral slopes $\alpha_{\rm OX}$ is 1.46 ± 0.01 for the NE nucleus and 2.32 ± 0.13 for the SW nucleus

(SI). The estimated unabsorbed hard X-ray (2–8 keV) luminosities (assuming a redshift of z = 2.17 for both X-ray point sources) are $\sim 10^{45.29^{+0.05}_{-0.03}}$ erg s^{-1} for the NE nucleus and $\sim 10^{43.62^{+0.32}_{-0.58}}$ erg s^{-1} for the SW nucleus, both greatly exceeding the most X-ray luminous starburst galaxies[12]. We also find significantly different intrinsic absorbing columns in the two nuclei ($4.7^{+1.3}_{-2.6} \times 10^{22}$ cm^{-2} for the NE nucleus and $<10^{20}$ cm^{-2} for the SW nucleus), lending further support to the dual quasar hypothesis.

Third, both quasar nuclei are detected as compact radio sources by *VLA* A-config continuum imaging at 6 GHz and 15 GHz (Figure 3). The radio point source centers are consistent with those of the *HST* optical quasar nuclei. The radio flux ratios between the two nuclei (NE/SW) are 0.379±0.001 at 6 GHz and 0.351±0.003 at 15 GHz, which are different (by $> 5\sigma$) than those observed by *HST* in the optical (0.229±0.001 in F475W and 0.284±0.002 in F814W), disfavoring strong lensing but with the caveat of flux ratio anomalies caused by microlensing. The radio spectral indices are -0.397 ± 0.004 for the NE nucleus and -0.314 ± 0.002 for the SW nucleus. The radio loudness parameter $R_{6\,cm/2500\,\mathring{A}}$, commonly defined as the flux density ratio at the rest-frame 6 cm and that at 2500 Å, is 1079±74 for the NE nucleus and 659±16 for the SW nucleus, placing both quasars in the radio-loud (i.e., $R_{6\,cm/2500\,\mathring{A}} > 10$) population according to the canonical definition[13].

Finally, *HST* spatially resolved optical spectroscopy shows significantly different rest-frame UV continuum spectral slopes between the two nuclei ($\alpha_\nu = -0.70\pm0.24$ for the NE nucleus and 0.08 ± 0.06 for the SW nucleus), independently confirmed by Gemini/GMOS spatially resolved optical slit spectroscopy (Figure 4). However, the GMOS spectra are only marginally resolved for the two nuclei and hence the spectral slope measurements are not as reliable as the HST-based results. The different spectral slopes disfavor a strongly lensed quasar, although strong gravitational lenses may also produce different spectral slopes due to varying reddening along different light paths through the foreground lens galaxy[14]. There are noticeable differences in the broad emission lines, but the low spectroscopic data quality cannot conclusively rule out strong lensing based on the line shapes alone. The best-fit systemic redshifts estimated from the optical-IR spectra of the two quasar nuclei suggest a line-of-sight velocity offset of $\sim310\pm50$ km s^{-1} (Supplementary Table 1 in SI), consistent with expectations of typical orbital velocities in galaxy mergers[15] but inconsistent with strong lensing (which would produce identical redshifts of the two quasars).

By modeling the PSF-subtracted, host-galaxy only, two-band (*HST* F160W and Keck AO K_p) photometry of SDSS J0749+2255, we estimate the stellar masses of the two host galaxies as $\sim10^{11.46^{+0.02}_{-0.26}}M_\odot$ and $\sim10^{11.50^{+0.04}_{-0.27}}M_\odot$ (with the errors accounting for the 1σ statistical and partial systematic uncertainties from surface brightness profile fitting but

ignoring additional systematics from population synthesis modeling) for the NE nucleus and the SW nucleus. The massive hosts appear to be compact and disk-dominated (with best-fit Sérsic indices close to unity; SI), typical of galaxies[16] and hosts of single quasars[17] at $z > 2$. The disk dominance of the hosts in SDSS J0749+2255 is dramatically different from the more bulge-dominated characteristics of low-redshift low-luminosity dual AGN hosts[18]. The latter may be more subject to the stabilization effect of stellar bulges preventing more efficient SMBH fueling in the early merging stages, resulting in low-luminosity AGNs rather than the luminous quasars observed in SDSS J0749+2255.

By jointly modeling the optical-NIR spectrum (SI), we estimate the SMBH masses as $\sim 10^{9.1\pm0.4} M_{\odot}$ and $\sim 10^{9.2\pm0.4} M_{\odot}$ (with the errors representing 1σ total uncertainties) for the NE and the SW nuclei. Bolometric luminosities estimated from the optical continua suggest Eddington ratios of $\sim 0.12 \pm 0.03$ and $\sim 0.25 \pm 0.07$ for the NE and SW nuclei, respectively. The SMBH masses and host total stellar masses are consistent with the empirical scaling relations observed in both single quasars at $z \sim 2$ and local inactive galaxies within uncertainties (SI).

SDSS J0749+2255 represents a robust example of a kpc-scale pair of SMBHs in a galaxy merger at cosmic noon. It fills a long-standing gap in the expected population of dual quasars hosted by high-redshift ongoing galaxy mergers. Such systems are expected

to be common in hierarchical merger models, which have been otherwise successful in explaining much of the quasar phenomenology[1]. In comparison, the previous redshift record holder of kpc-scale dual quasars hosted by confirmed galaxy mergers was LBQS 0103−2753 at $z = 0.86$, which was serendipitously discovered[19].

A handful of galactic-scale (< 10 kpc) dual quasar candidates were known at $z > 1$[7,20–27]. However, none of them has been confirmed to be hosted by ongoing galaxy mergers – as expected in bona fide dual quasars (SI). The establishment of SDSS J0749+2255 as a dual quasar hosted in a galaxy merger conclusively demonstrates that at least some high-redshift kpc-scale dual quasar candidates may indeed be dual quasars rather than gravitational lenses or pre-merger projected quasar pairs at large separations. On larger (i.e., > 10 kpc) scales, it has long been suggested that most wide separation (3″–10″) double quasars are quasar pairs rather than gravitational lenses based on statistical arguments[28]. There are ∼tens of known "binary" quasars at $z > 1$ with projected separations of > 10 kpc[29] and even a quasar "quartet"[30]. However, the separations of most of these systems are still too large ($\gtrsim$ tens of kpc) for the host galaxies of the quasar pair to be in direct galactic interactions. Unlike SDSS J0749+2255, none of them has been observed with tidal features as direct evidence for ongoing interactions.

Despite significant merit and intense theoretical interest, direct evidence for compact

binary SMBHs – SMBHs that are gravitationally bound to each other – is still lacking[2]. Their separations (typically less than a few parsecs) are too small to resolve beyond the local universe with current facilities. High-redshift kpc-scale dual quasars represent promising progenitors of low-redshift compact binary SMBHs. Using a stellar dynamical friction argument, we estimate that the 3.8 kpc SMBH pair in SDSS J0749+2255 may form a compact bound SMBH binary in $\lesssim 0.22^{+0.50}_{-0.16}$ Gyr (SI). Future infrared integral field unit spectroscopy with the James Webb Space Telescope will map the stellar and gas kinematics, enabling better predictions on the subsequent SMBH pair orbital evolution and the impact of dual quasar on their host galaxies.

The confirmation of SDSS J0749+2255 as a dual quasar provides a proof-of-concept for combining multi-wavelength facilities to discover high-redshift kpc-scale dual quasars[7]. The discovery underscores the need for high-resolution deep NIR imaging, which is crucial for detecting the merging galaxy hosts and for robustly distinguishing high-redshift dual quasars from lensed quasars and pre-merger projected quasar pairs at larger physical separations. Future high-resolution wide-area deep surveys will uncover a larger sample of high-redshift dual quasars at the peak epoch of galaxy and SMBH assembly.

1. Hopkins, P. F., Hernquist, L., Cox, T. J. & Kereš, D. A Cosmological Framework for the Co-Evolution of Quasars, Supermassive Black Holes, and Elliptical Galaxies. I.

Galaxy Mergers and Quasar Activity. *Astrophys. J. Suppl. Ser.* **175**, 356–389 (2008).

2. Bogdanović, T., Miller, M. C. & Blecha, L. Electromagnetic counterparts to massive black-hole mergers. *Living Rev. Relativ.* **25**, 3 (2022).

3. Richards, G. T. *et al.* The Sloan Digital Sky Survey Quasar Survey: Quasar Luminosity Function from Data Release 3. *Astron. J.* **131**, 2766–2787 (2006).

4. Madau, P. & Dickinson, M. Cosmic Star-Formation History. *Annu. Rev. Astro. Astrophys.* **52**, 415–486 (2014).

5. Schneider, D. P. *et al.* The Sloan Digital Sky Survey Quasar Catalog. V. Seventh Data Release. *Astron. J.* **139**, 2360–2373 (2010).

6. Hwang, H.-C., Shen, Y., Zakamska, N. & Liu, X. Varstrometry for Off-nucleus and Dual Subkiloparsec AGN (VODKA): Methodology and Initial Results with Gaia DR2. *Astrophys. J.* **888**, 73 (2020).

7. Shen, Y. *et al.* A hidden population of high-redshift double quasars unveiled by astrometry. *Nat. Astron.* **5**, 569–574 (2021).

8. Barnacka, A., Geller, M. J., Dell'Antonio, I. P. & Benbow, W. Strong Gravitational Lensing as a Tool to Investigate the Structure of Jets at High Energies. *Astrophys. J.* **788**, 139 (2014).

9. Chang, K. & Refsdal, S. Flux variations of QSO 0957 + 561 A, B and image splitting by stars near the light path. *Nature* **282**, 561–564 (1979).

10. Wambsganss, J. & Paczynski, B. Expected Color Variations of the Gravitationally Microlensed QSO 2237+0305. *Astron. J.* **102**, 864–868 (1991).

11. Pooley, D., Blackburne, J. A., Rappaport, S., Schechter, P. L. & Fong, W.-f. A Strong X-Ray Flux Ratio Anomaly in the Quadruply Lensed Quasar PG 1115+080. *Astrophys. J.* **648**, 67–72 (2006).

12. Zezas, A., Alonso-Herrero, A. & Ward, M. J. Searching for X-Ray Luminous Starburst Galaxies. *Astrophys. Space Sci.* **276**, 601–607 (2001).

13. Kellermann, K. I., Sramek, R., Schmidt, M., Shaffer, D. B. & Green, R. VLA Observations of Objects in the Palomar Bright Quasar Survey. *Astron. J.* **98**, 1195–1207 (1989).

14. Sluse, D., Hutsemékers, D., Courbin, F., Meylan, G. & Wambsganss, J. Microlensing of the broad line region in 17 lensed quasars. *Astron. Astrophys.* **544**, A62 (2012).

15. Contreras-Santos, A. *et al.* Galaxy pairs in THE THREE HUNDRED simulations: a study on the performance of observational pair-finding techniques. *Mon. Not. R. Astron. Soc.* **515**, 5375–5388 (2022).

16. Shapley, A. E. Physical Properties of Galaxies from z = 2 to 4. *Annu. Rev. Astron. Astrophys.* **49**, 525–580 (2011).

17. Ding, X., Silverman, J. D. & Onoue, M. Opening the Era of Quasar-host Studies at High Redshift with JWST. *Astrophys. J. Lett.* **939**, L28 (2022).

18. Shangguan, J. *et al.* Chandra X-Ray and Hubble Space Telescope Imaging of Optically Selected Kiloparsec-scale Binary Active Galactic Nuclei. II. Host Galaxy Morphology and AGN Activity. *Astrophys. J.* **823**, 50 (2016).

19. Shields, G. A. *et al.* LBQS 0103-2753: A Binary Quasar in a Major Merger. *Astrophys. J.* **744**, 151 (2012).

20. Inada, N. *et al.* The Sloan Digital Sky Survey Quasar Lens Search. II. Statistical Lens Sample from the Third Data Release. *Astron. J.* **135**, 496–511 (2008).

21. Schechter, P. L. *et al.* First Lensed Quasar Systems from the VST-ATLAS Survey: One Quad, Two Doubles, and Two Pairs of Lensless Twins. *Astron. J.* **153**, 219 (2017).

22. Anguita, T. *et al.* The STRong lensing Insights into the Dark Energy Survey (STRIDES) 2016 follow-up campaign - II. New quasar lenses from double component fitting. *Mon. Not. R. Astron. Soc.* **480**, 5017–5028 (2018).

23. Lemon, C. A., Auger, M. W., McMahon, R. G. & Ostrovski, F. Gravitationally lensed quasars in Gaia - II. Discovery of 24 lensed quasars. *Mon. Not. R. Astron. Soc.* **479**, 5060–5074 (2018).

24. Lemon, C. *et al.* The STRong lensing Insights into the Dark Energy Survey (STRIDES) 2017/2018 follow-up campaign: discovery of 10 lensed quasars and 10 quasar pairs. *Mon. Not. R. Astron. Soc.* **494**, 3491–3511 (2020).

25. Tang, S. *et al.* Optical Spectroscopy of Dual Quasar Candidates from the Subaru HSC-SSP program. *Astrophys. J.* **922**, 83 (2021).

26. Yue, M., Fan, X., Yang, J. & Wang, F. A Candidate Kiloparsec-scale Quasar Pair at z = 5.66. *Astrophys. J. Lett.* **921**, L27 (2021).

27. Lemon, C. *et al.* J1721+8842: a gravitationally lensed binary quasar with a proximate damped Lyman-α absorber. *Astron. Astrophys.* **657**, A113 (2022).

28. Kochanek, C. S., Falco, E. E. & Muñoz, J. A. Why Quasar Pairs are Binary Quasars and Not Gravitational Lenses. *Astrophys. J.* **510**, 590–596 (1999).

29. Hennawi, J. F. *et al.* Binary Quasars at High Redshift. I. 24 New Quasar Pairs at z ˜ 3-4. *Astrophys. J.* **719**, 1672–1692 (2010).

30. Hennawi, J. F., Prochaska, J. X., Cantalupo, S. & Arrigoni-Battaia, F. Quasar quartet embedded in giant nebula reveals rare massive structure in distant universe. *Science* **348**, 779–783 (2015).

31. Peng, C. Y., Ho, L. C., Impey, C. D. & Rix, H.-W. Detailed Decomposition of Galaxy Images. II. Beyond Axisymmetric Models. *Astron. J.* **139**, 2097–2129 (2010).

Acknowledgements We thank the anonymous referees for the constructive reports that helped improve the presentation of this work. We thank A. Kemball and A. Gross for helpful discussions on strong lensing. We thank M. Leveille, A. Vick, R. Campbell, R. McGurk, J. Cortes, T. R. Geballe, S. Leggett, A. Nitta, T. Seccull, and H. Medlin for their help with our HST, Keck, Gemini, and VLA observations. Y.-C.C. thanks J. Li and H. Guo for their help with the GALFIT and PyQSOFit codes. M.O. acknowledges support from JSPS KAKENHI grants JP20H00181, JP20H05856, JP22H01260. This work is supported by the Heising-Simons Foundation and Research Corporation for Science Advancement and NSF grants AST-2108162 and AST-2206499. This research was supported in part by the National Science Foundation under PHY-1748958. Support for Program number 23700237 was provided by NASA through Chandra Award Number GO2-23099X issued by the Chandra X-ray Observatory Center, which is operated by the Smithsonian Astrophysical Observatory for and on behalf of NASA under contract NAS 8-03060. Support for Program number HST-GO-15900 (PI: H. Hwang), HST-GO-16210, and HST-GO-16892 was provided by NASA through grants from the Space Telescope Science Institute, which is operated

by the Association of Universities for Research in Astronomy, Incorporated, under NASA contract NAS5-26555. The National Radio Astronomy Observatory is a facility of the National Science Foundation operated under cooperative agreement by Associated Universities, Inc. Based in part on data obtained at the W. M. Keck Observatory, which is operated as a scientific partnership among the California Institute of Technology, the University of California and the National Aeronautics and Space Administration. The Observatory was made possible by the generous financial support of the W. M. Keck Foundation. This research has made use of the Keck Observatory Archive (KOA), which is operated by the W. M. Keck Observatory and the NASA Exoplanet Science Institute (NExScI), under contract with the National Aeronautics and Space Administration. The authors wish to recognize and acknowledge the very significant cultural role and reverence that the summit of Maunakea has always had within the indigenous Hawaiian community. We are most fortunate to have the opportunity to conduct observations from this mountain. Based in part on observations obtained at the international Gemini Observatory (Program IDs 2020B-FT-113 and GN-2022A-Q-139; PI: X. Liu), a program of NSF's NOIRLab, which is managed by the Association of Universities for Research in Astronomy (AURA) under a cooperative agreement with the National Science Foundation. on behalf of the Gemini Observatory partnership: the National Science Foundation (United States), National Research Council (Canada), Agencia Nacional de Investigación y Desarrollo (Chile), Ministerio de Ciencia, Tecnología e Innovación (Argentina), Ministério da Ciência, Tecnologia, Inovações e Comunicações (Brazil), and Korea Astronomy and Space Science Institute (Republic of Korea). This work was enabled by observations made from the Gemini North telescope, located within the Maunakea Science Reserve and adjacent to the

summit of Maunakea. We are grateful for the privilege of observing the Universe from a place that is unique in both its astronomical quality and its cultural significance. This work makes use of SDSS-I/II and SDSS-III/IV data (http://www.sdss.org/ and http://www.sdss3.org/).

Author Contributions Y.-C.C. conducted the VLA and Keck observations, reduced and analyzed the *HST*, Gemini, and VLA data, performed the GALFIT analysis and the optical and NIR spectroscopic modeling. X.L. led the study, was PI of the Chandra, Gemini, *HST*, and VLA observing programs, conducted the Keck observations, and reduced the Keck data. A.F. analyzed the Chandra data and performed the `BAYMAX` analysis. Y.S. was PI of the Keck observing program, conducted the Keck observations, and wrote the optical and NIR spectroscopic modeling pipeline. M.O. performed the strong lensing mass model tests. N.C. performed the cosmological simulations. X.L., Y.-C.C., A.F., and Y.S. co-wrote the manuscript with the help of N.C. and M.H.. All authors contributed to the results and commented on the manuscript.

Author Information Reprints and permissions information is available at www.nature.com/reprints. The authors declare no competing financial interests. Publisher's note: Springer Nature remains neutral with regard to jurisdictional claims in published maps and institutional affiliations. Correspondence and requests for materials should be addressed to X.L. (xinliuxl@illinois.edu).

Code availability The code used to model the *HST* and Keck data is publicly available at https://users.obs.carnegiescience.edu/peng/work/galfit/galfit.html. The code used for

the lensing mass modeling test is publicly available at https://github.com/oguri/glafic2. The code used to perform the optical-NIR spectroscopic analysis is publicly available at https://github.com/legolason/PyQSOFit. The BAYMAX code used to model the Chandra data is available upon reasonable request.

Data availability The SDSS spectrum (Plate = 1203, FiberID = 576, MJD = 52669) is publicly available at https://www.sdss.org/. The HST, Chandra, VLA, Gemini, and Keck data are all available through their separate public data archives (HST program numbers GO-16210 and GO-16892, Chandra GO-23700377, VLA 20B-242, Gemini 2020B-FT-113 and 2022A-Q-139).

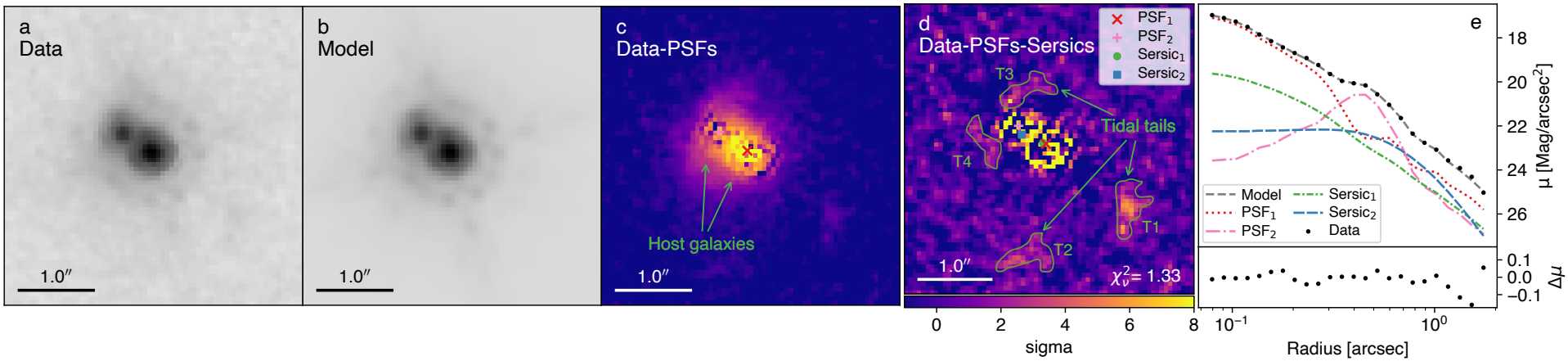

Figure 1: **HST imaging.** HST/WFC3 F160W (H band) image and 2D structural decomposition results using GALFIT[31] modeling for SDSS J0749+2255. Panel a: the raw HST image; Panel b: our best-fit model consisting of two PSFs for the central quasars and two Sérsic models for the two host galaxies; Panel c: the two-PSF-subtracted image highlighting the detection of two host galaxies underlying both quasars in the merger; Panel d: the residual image after subtracting two PSFs and two Sérsic models finally revealing the detection of low surface-brightness tidal tails indicative of ongoing galactic interactions; and Panel e: the 1D radial profiles of the data and the best-fit model and the individual components. The detection of both the host galaxies and the tidal tails unambiguously confirms the system as a dual quasar rather than a lensed quasar or a pre-merger projected quasar pair at larger physical separations. In addition to the two Sérsic models for the two quasar host galaxies, we have also considered the alternative scenario of a single Sérsic model for a central foreground lens galaxy which is disfavored by the data based on the χ^2_ν values.

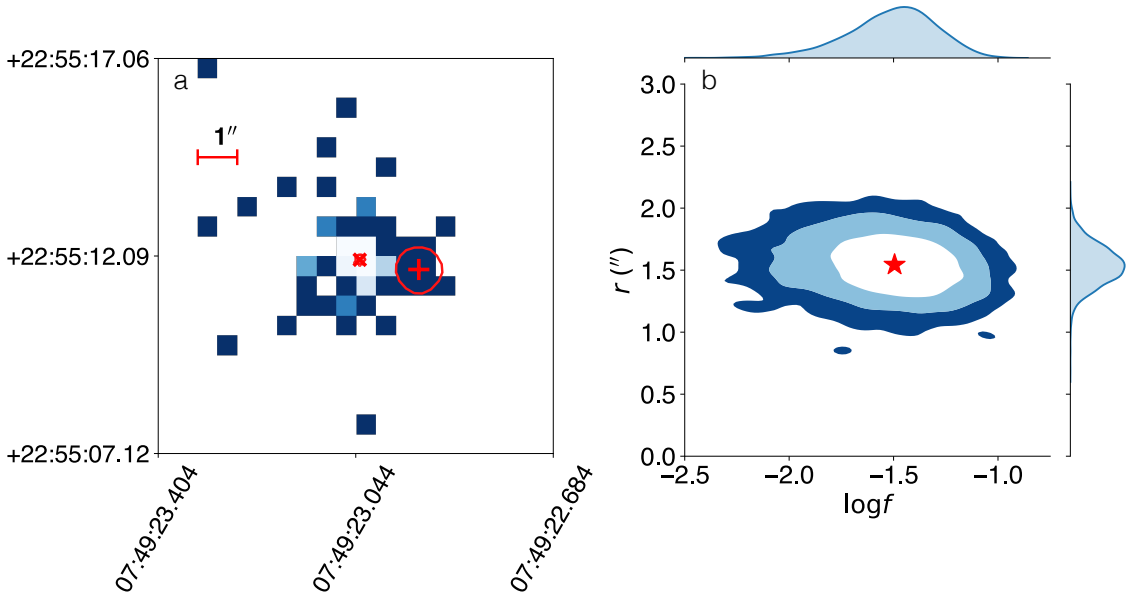

Figure 2: **X-ray imaging.** *Chandra* ACIS-S X-ray image and best-fit BAYMAX results for SDSS J0749+2255. Panel a shows binned *Chandra* data (0.5−8 keV), centered on the nominal X-ray coordinates of quasar with best-fit location of primary X-ray point source (red "x") and secondary X-ray point source (red "+") with 95% confidence interval shown in red contour; Panel b shows joint-posterior distribution of the separation (r, in arcsecond) and count ratio (log f; ratio between the number of counts associated with secondary versus the primary). Blue contour levels represent 68%, and 95% confidence intervals. We find the best-fit separation $r = 1\farcs54^{+0\farcs39}_{-0\farcs36}$ and $\log f = -1.43^{+0.30}_{-0.30}$, at the 95% confidence interval. Although the estimated separation is statistically larger than estimated from *HST* imaging ($0\farcs46$), the estimated position angle between the two X-ray point sources (350^{+37}_{-24} deg.; 95% confidence interval) is consistent with the position angle of the two resolved cores resolved in the *HST* imaging (330 deg.).

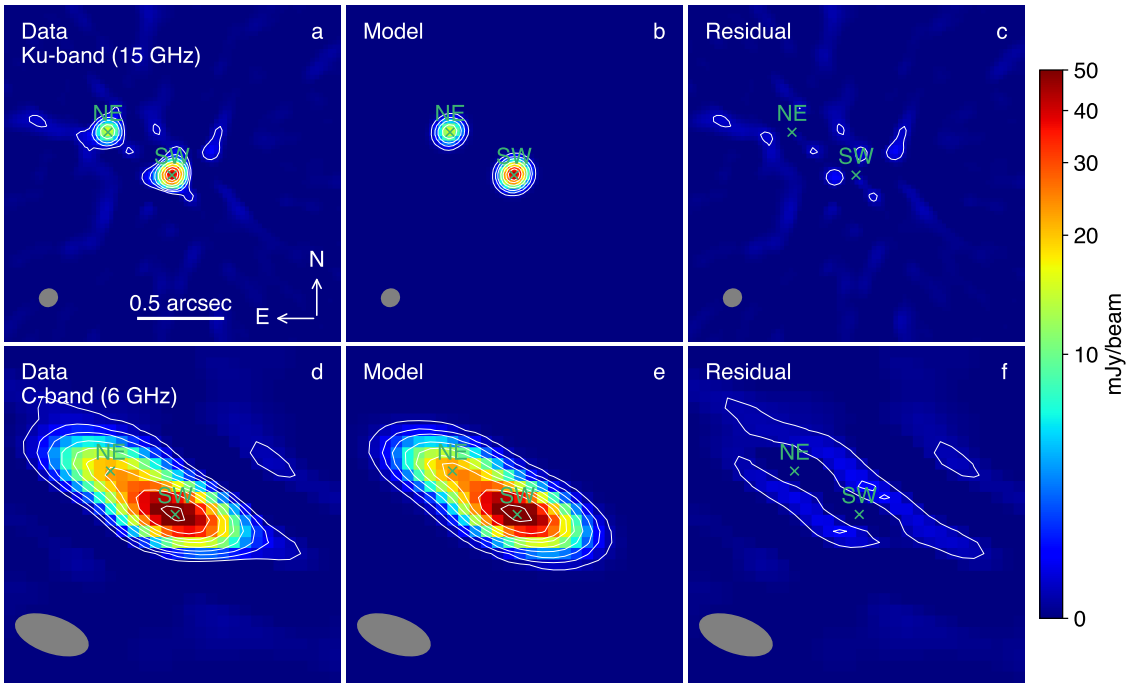

Figure 3: **Radio imaging.** VLA A-config Ku-band (Panel a) and C-band (Panel d) continuum images for SDSS J0749+2255. Panels b and c (e and f) show the Ku-band (C-band) model and residual images. The contours represent 10, 30, 60, 120, 200, 300, 400, 600, 1000 $\times$ 1σ noise levels. The green crosses mark the centroids of the fitted Gaussian components. The synthesized beam sizes are shown in grey in the bottom left corner. The restoring beam sizes are $0\farcs11\times$ $0\farcs10$ (PA=-54.0 deg) in the Ku band and $0\farcs44\times0\farcs21$ (PA=70.9 deg) in the C band. The rms noise levels are 8.2 μJy beam^{-1} in the Ku band and 5.3 μJy beam^{-1} in the C band.

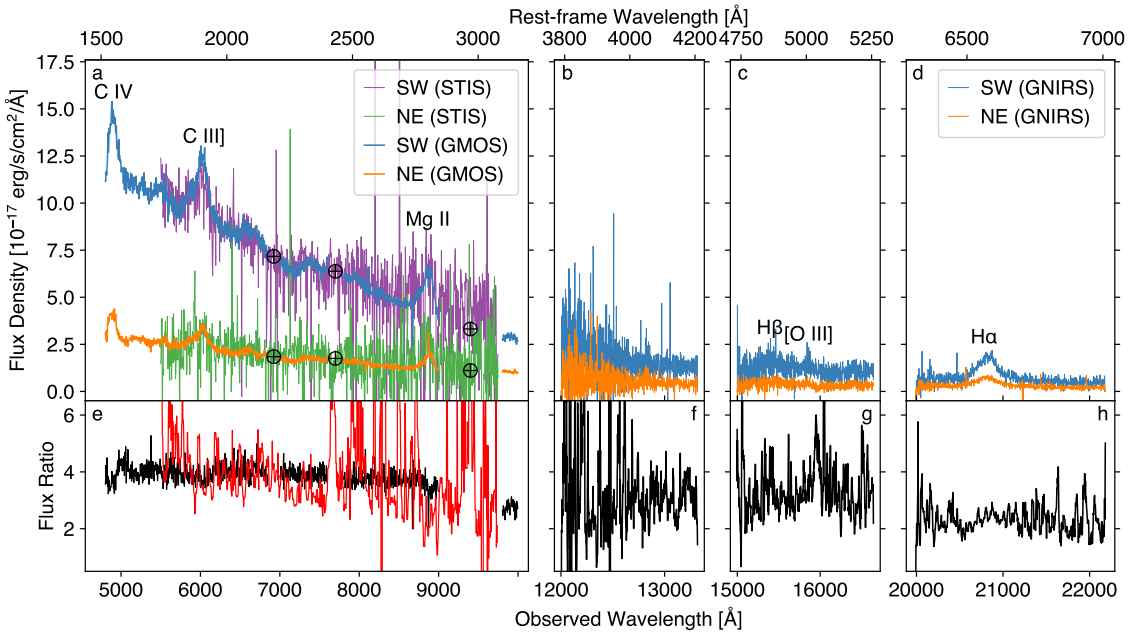

Figure 4: **Optical and near-infrared spectroscopy.** Panels a–d: Spatially resolved optical and NIR spectroscopy from *HST*/STIS, Gemini/GMOS, and Gemini/GNIRS for SDSS J0749+2255. The orange and cyan curves represent Gemini spectra for the northeastern (NE) and southwestern (SW) nuclei, respectively. The green and magenta curves show the *HST* spectra for the NE and SW nuclei. Labeled are the detected major strong emission lines. The circled-cross symbols exhibit the telluric absorption region. Panels e–h: Flux ratios between the two nuclei, where the *HST*-based flux ratio is shown in red and the Gemini-based flux ratio (for both GMOS and GNIRS) is shown in black. The two nuclei have significantly different rest-frame UV continuum spectral slopes and strengths of the broad and narrow emission lines. The discrepancy between the STIS- and GMOS-based flux ratios is likely cause by differences in the slit coverage and/or observing time. We adopt the STIS spectra to estimate the continuum power-law spectral indices because STIS cleanly separated the two nuclei.